



MAX-PLANCK-GESELLSCHAFT

Lihong Feng    Jan G Korvink    Peter Benner

**A Fully Adaptive Scheme for Model Order  
Reduction Based on Moment-matching**



**Max Planck Institute Magdeburg  
Preprints**

MPIMD/12-14

September 6, 2012

**Impressum:**

**Max Planck Institute for Dynamics of Complex Technical Systems, Magdeburg**

**Publisher:**

Max Planck Institute for Dynamics of Complex  
Technical Systems

**Address:**

Max Planck Institute for Dynamics of  
Complex Technical Systems  
Sandtorstr. 1  
39106 Magdeburg

[www.mpi-magdeburg.mpg.de/preprints](http://www.mpi-magdeburg.mpg.de/preprints)



MAX-PLANCK-GESELLSCHAFT

# Max Planck Institute Magdeburg Preprints

Lihong Feng    Jan G Korvink    Peter Benner

## A Fully Adaptive Scheme for Model Order Reduction Based on Moment-matching



# A Fully Adaptive Scheme for Model Order Reduction Based on Moment-matching

Lihong Feng\*      Jan G. Korvink<sup>†</sup>      Peter Benner<sup>‡</sup>

September 6, 2012

## Abstract

A fully adaptive model order reduction scheme based on moment-matching is proposed to derive the reduced model of a linear time invariant system. According to the given error tolerance, the order of the reduced model, as well as the expansion points for the transfer function, are automatically determined on the fly during the process of model reduction. In this sense, the reduced model is automatically obtained without heuristically assigning the number of moments and expansion points before model reduction, which is a prerequisite for the standard implementation of model reduction based on moment matching. The proposed adaptive scheme is found to be efficient when it is tested on various linear time invariant systems.

## 1 Introduction

Model order reduction (MOR) for linear time invariant (LTI) systems has demonstrated great efficiency in the simulation of large-scale systems. Model reduction methods based on balanced truncation are very efficient for medium to large-scale problems [1, 2]. It is well known that a global error bound for the reduced model makes the model reduction process automatic. Although model reduction methods based on Krylov subspace and moment-matching are much simpler to be implemented and also require much less computational complexity than methods based on balanced truncation, they cannot be performed adaptively. One always has to decide, by experience or heuristically, the number of moments to be matched and the position of the expansion points to be used for the transfer function. In this case, one runs

---

\*Lihong Feng is with Max Planck Institute for Dynamics of Complex Technical Systems, Germany. [feng@mpi-magdeburg.mpg.de](mailto:feng@mpi-magdeburg.mpg.de)

<sup>†</sup>Jan G. Korvink is with Department of Microsystems Engineering (IMTEK) and Freiburg Institute of Advanced Studies (FRIAS), University of Freiburg, Germany. [korvink@imtek.uni-freiburg.de](mailto:korvink@imtek.uni-freiburg.de)

<sup>‡</sup>Peter Benner is with Max Planck Institute for Dynamics of Complex Technical Systems and Faculty of Mathematics, Chemnitz University of Technology, Germany. [benner@mpi-magdeburg.mpg.de](mailto:benner@mpi-magdeburg.mpg.de)

the risk of performing model reduction repeatedly before a satisfactory solution is found. The worst case is that, after several attempts, the reduced model remains inaccurate. The most difficult task is choosing suitable expansion points, and in many cases using only an expansion point at zero is not sufficient for an accurate and small reduced model. However, how to choose proper nonzero expansion points and how to decide upon the corresponding number of moments accordingly is still unknown. The above problems are therefore the most tricky issues for model reduction based on moment-matching.

Until now, this area of research has barely been touched upon and the problems above still remain open. An early method called CFH (Complex Frequency Hopping) is proposed in [3] to illustrate a principle of choosing multiple expansion points of the transfer function. By using a binary search algorithm, the expansion points are chosen with respect to the common poles contained in both circles of the neighboring expansion points. However, the poles of the transfer function are computed based on explicit moment-matching. This means that the moments which are needed to compute the poles are explicitly computed by recursive matrix-vector multiplications, in the same way as the Asymptotic Waveform Evaluation method in [4]. Therefore, the poles computed are actually not accurate, because of numerical instability, although they would represent the actual poles if computed with precise arithmetic. Moreover, in order to compute the actual poles according to the theorem of convergence (Theorem 1 in [4]), higher order moments must be computed. However, explicit moment computation cannot guarantee that the higher order moments are accurately computed, again because of numerical instability. Usually, at most the first 20 moments can be accurately computed. A transfer-function-based approach is proposed in [5] by using a similar binary search algorithm as in [3]. However, one reduced model is constructed at each expansion point, which means 10 reduced models are constructed if 10 expansion points are chosen. Furthermore, the reduced models are obtained by explicitly calculating the moments, which is not numerically stable.

Recently, the issue of multi-point expansion for the transfer function is readdressed in [6]. Methods based on interpolation are proposed in the paper, which claim some rules for selecting the interpolation points needed for approximating the transfer function. However, these methods are rather limited for the task at hand. For example, the methods are actually not adaptive in choosing the number of the interpolation points, and may be implemented only after a fixed number is given.

In this paper we aim at solving the above open problems for model reduction of LTI systems. Our method is based on a bisection principle used to adaptively choose the expansion points for the transfer function, which is very similar to the binary technique used in [3, 5]. The differences from the algorithms of [3, 5] may be summarized as follows. Firstly, a single reduced model can be obtained by our method as compared with the method in [5]. Secondly, a different stopping criterion is used. Thirdly, the error estimation of the reduced model is the error between the reduced model and the original model, which can be computed cheaply. Fourthly, the expansion points are chosen to compute the projection matrix  $V$  based on implicit moment-matching [7], which can maintain numerical stability. The proposed method not only provides an adaptive scheme for selecting the expansion points, but also tells us how to adaptively choose the moments for each expansion point, as well as a proper order of the reduced model, something which cannot be adaptively selected by the previous methods.

We review the standard moment matching model reduction method PRIMA [7] in the next section. In Section 3, the key ideas of our adaptive scheme are described, and the implementa-

tion details are discussed as well. Simulation results for several examples in Integrated Circuit (IC) interconnect design are presented in Section 4.

## 2 Review of MOR based on moment-matching

Among the various model reduction methods based on moment matching, the basic methods for linear systems include those described in [7, 8]. Since the method PRIMA in [7] preserves the passivity of the original system, it is usually the method of choice for model order reduction of linear systems. Our adaptive scheme is based on PRIMA and aims to obtain the reduced model of the linear descriptor system

$$\begin{aligned} C \frac{d}{dt}x(t) + Gx(t) &= Bu(t), \\ y(t) &= L^T x(t). \end{aligned} \quad (1)$$

Such systems arise from, e.g., the modelling of interconnects in IC design, and of coupled field problems in MEMS simulation, mainly from discretized partial differential equations (PDEs) obtained via a finite element discretization, a PEEC discretization, or the method of moments. Here,  $x(t) \in \mathbb{R}^n$  is the state vector,  $u(t) \in \mathbb{R}^{m_1}$  is the input signal and  $y(t) \in \mathbb{R}^{m_2}$  is the output response. We consider general multi-input and multi-output systems, i.e.  $m_1 \geq 1$  and  $m_2 \geq 1$ .

Many model reduction methods are based on the idea of projection, i.e. a basis of a subspace which approximates the manifold in which the state vector  $x(t)$  resides is first computed, and then the reduced order model is obtained by Petrov-Galerkin projection. If we use system (1) as an example, usually a matrix  $V \in \mathbb{R}^{n \times r}$  whose columns span the subspace is computed, such that  $x(t)$  is approximated by its projection onto the subspace, i.e.,  $x(t) \approx Vz(t)$ ,

$$\begin{aligned} CV \frac{d}{dt}z(t) + GVz(t) &\approx Bu(t), \\ y(t) &\approx L^T Vz(t). \end{aligned} \quad (2)$$

The reduced model is derived by forcing the residual  $e = CV \frac{d}{dt}z(t) + GVz(t) - Bu(t)$  of the above first equation to be zero in a subspace which is spanned by the columns of a matrix  $W \in \mathbb{R}^{n \times r}$ , i.e.,

$$\begin{aligned} W^T CV \frac{d}{dt}z(t) + W^T GVz(t) &= W^T Bu(t), \\ y(t) &= L^T Vz(t). \end{aligned} \quad (3)$$

The above process in (3) associated with  $W$  is the so-called Petrov-Galerkin projection. The variable  $r \leq n$  indicates the dimension of system (3), which is also called the order of the reduced model. Model reduction methods based on projection differ in the computation of the matrices  $W$  and  $V$ . Methods related to balanced truncation [1, 2] compute  $W, V$  according to the Gramians of the system, whereas methods based on moment-matching compute  $W, V$  according to the series expansion of the transfer function.

In order to preserve the passivity of the original system, PRIMA [7] uses  $W = V$  such that the reduced model is guaranteed to be passive if the original system is passive. The matrix  $V$  is constructed from the moments of the transfer function (matrix),

$$Y(s) = H(s)U(s) = L^T (sC + G)^{-1} BU(s). \quad (4)$$

and

$$H(s) = L^T(sC + G)^{-1}B. \quad (5)$$

$H(s)$  is derived from the Laplace transform of (1). The Laplace domain variable  $s$  is related to frequency  $f$  by  $s = 2\pi jf$

If we expand  $H(s)$  around some expansion point  $s_0$  as

$$\begin{aligned} H(s) &= L^T[(s - s_0 + s_0)C + G]^{-1}B \\ &= L^T[(s - s_0)C + (s_0C + G)]^{-1}B \\ &= L^T[I + (s_0C + G)^{-1}C(s - s_0)]^{-1}(s_0C + G)^{-1}B \\ &= \sum_{i=0}^{\infty} \underbrace{L^T[-(s_0C + G)^{-1}C]^i (s_0C + G)^{-1}B}_{:=m_i(s_0)} (s - s_0)^i, \end{aligned}$$

then  $m_i(s_0)$ ,  $i = 0, 1, 2, \dots$  are called the  $i$ th order moments of the transfer function  $H(s)$ . The columns of  $V$  span the subspace

$$\text{range}\{V\} = \text{span}\{\tilde{B}(s_0), (\tilde{G}(s_0)^{-1}C)\tilde{B}(s_0), \dots, (\tilde{G}(s_0)^{-1}C)^q\tilde{B}(s_0)\}, \quad (6)$$

where  $\tilde{G}(s_0) = s_0C + G$ ,  $\tilde{B}(s_0) = (s_0C + G)^{-1}B$ . In this paper we call  $(\tilde{G}(s_0)^{-1}C)^i\tilde{B}(s_0)$ ,  $i = 0, 1, \dots$  the  $i$ th order moment vectors.

It is proved in [7] that the first  $q + 1$  moments of the (reduced) transfer function of the reduced model are the same as those corresponding moments of the original transfer function  $H(s)$ , i.e.

$$H_r(s) - H(s) = o(s - s_0)^q. \quad (7)$$

Here,  $H_r(s)$  is the reduced transfer function. It implies that, for a fixed  $s_0$ , a larger  $q$  produces a more accurate  $H_r(s)$ .

From (7) one can see that the accuracy of  $H_r$  also depends on  $s_0$ . For a fixed  $q$ , if  $s'$  is far away from  $s_0$ , the error of  $H_r$  at  $s'$  is usually larger than for those variables that are close to  $s_0$ . This implies that if  $s_0$  is chosen as zero, then  $H_r(s)$  is probably not accurate at high frequencies where  $f \gg f_0$ . One may also use multi expansion points to overcome the large error caused at high frequencies. However, it is not immediately clear how to choose suitable expansion points, or indeed how many corresponding moments should be taken. For the current model reduction methods based on moment-matching, the two variables  $s_0$  and  $q$  are heuristically given a priori, because there is not a general rule for properly choosing them.

### 3 The adaptive scheme

A smart technique of automatically choosing the number of moments, as well as the expansion points, is proposed in this section. To make the procedure clear, we first explain the adaptive scheme of matching moments given a single expansion point in subsection 3.1. Then, in the following subsection, we show the scheme of adaptively choosing both the expansion points and the corresponding number of moments, as well as the proper order  $r$  of the reduced model.

### 3.1 Adaptively choosing moments

As is known, given an interval of frequency  $f \in [f_l, f_h]$ , the range of the variable  $s$  is defined by  $s \in [s_l, s_h] := 2\pi j[f_l, f_h]$ . In this subsection, we only consider the adaptive choice of the number of moments associated with a single expansion point. For example, the transfer function is expanded around  $s_0$ .

From (7), we see that  $H_r(s)$  has its smallest error at  $s_0$ , and that the largest error must be contributed by a point  $s'$  which is far away from  $s_0$ . For two different variables  $s_1$  and  $s_2$  with  $|s_1 - s_0| < |s_2 - s_0|$ , we cannot say that  $error(s_1) = \|H(s_1) - H_r(s_1)\|/\|H(s_1)\|$  is also smaller than  $error(s_2) = \|H(s_2) - H_r(s_2)\|/\|H(s_2)\|$ . Here  $\|\cdot\|$  is a general description, we will give the detailed definition in Section 4 for SISO and MIMO systems separately.

However, if  $s_2$  is much farther away from  $s_0$  than  $s_1$ , and  $q$  is relatively large, the chance of  $error(s_2)$  being larger than  $error(s_1)$  increases. Since we never know how much farther  $s_2$  is than  $s_1$ , and how large  $q$  should be, we simply assume that the point  $s^*$  which is farthest away from  $s_0$  usually has the largest error for each  $q$ . Therefore, during MOR, we only check the error at  $s^*$  if we only use single point expansion. This is somehow heuristic, nevertheless, after many tests, we have found that the error at  $s^*$  can control the error over the entire range  $[s_l, s_h]$ . Although in many situations, especially when  $q$  is small, the largest error over  $[s_l, s_h]$  is not exactly at  $s^*$ , it has a similar magnitude as the error at  $s^*$ , i.e., the largest error is  $O(error(s^*))$ . Moreover, the point with the largest error is very close to  $s^*$  after a certain number  $q$  of moments are matched.

Based on this observation, the projection matrix  $V$  can be computed adaptively as follows.

#### Adaptive scheme of choosing moments:

M1: As input we specify the acceptable accuracy of the reduced model  $tol$ .  $tol$  here means the acceptable maximal relative error  $\max_{s \in [s_l, s_h]} \|H(s) - H_r(s)\|_2 / \|H(s)\|_2$  between the reduced transfer function and the original transfer function.

M2: The first moment vector  $\tilde{B}(s_0)$  is chosen, the projection matrix  $V$  is computed such that  $\text{range}\{V\} = \text{span}\{\tilde{B}(s_0)\}$ . Assume  $s^* \in [s_l, s_h]$  is the variable which is farthest away from  $s_0$  ( $s^*$  can be taken as e.g.  $s_h$  if  $s_0 = s_l$ ). Compute the reduced transfer function  $H_r(s^*)$  and the error  $\varepsilon(s^*) = \|H(s^*) - H_r(s^*)\|/\|H(s^*)\|$ .

M3: For  $i = 1, 2, \dots$ , while  $\varepsilon > tol$ , add new moment vectors  $(G(s_0)^{-1}C(s_0))^i \tilde{B}(s_0)$  to  $V$ , such that

$$\text{range}\{V\} = \text{span}\{\tilde{B}(s_0), (\tilde{G}(s_0)^{-1}C)\tilde{B}(s_0), \dots, (\tilde{G}(s_0)^{-1}C)^i \tilde{B}(s_0)\}$$

compute  $H_r(s^*)$  and  $\varepsilon$ , until  $\varepsilon < tol$ .

From the above steps, we see that at each iteration step  $i$ , only the error at the point  $s^*$  is checked, and usually this is sufficient. This is because if the error  $\varepsilon(s^*)$  at  $s^*$  is smaller than  $tol$ , the error  $\varepsilon(s')$  at  $s'$  (which causes the largest error in  $[s_l, s_h]$ ) is also small enough in many cases. In case there are exceptions, and in order to be more confident that  $\varepsilon(s')$  is also smaller than  $tol$ , one can take  $tol$  to be smaller (e.g. 10 times smaller) than the expected accuracy for the reduced model.

When the original system is very large and LU factorization of  $\tilde{G}(s_i)$  is not applicable due to memory limitations, all of the moment vectors of any expansion point  $s_i$  have to be computed by solving the linear systems  $\tilde{G}(s_i)^{-1}x = f$  with iterative methods, such as GMRES. The right hand side vector  $f$  may be the latest computed column of the matrix  $V$ . For such cases, computation of the original transfer function at one frequency point  $s^*$  is equivalent to the computation of one additional moment vector in (6). Therefore, the above error check is computationally reasonable.

For those systems with very sparse system matrices, so that the LU factorization of  $\tilde{G}(s_i)$  can be obtained more easily, the computation of the original transfer function at one frequency point  $s^*$  needs an extra LU factorization of  $\tilde{G}(s^*)$ , which is more expensive than computing one additional moment vector corresponding to the current expansion point  $s_i$ . However, the extra computation is still acceptable.

Once  $H(s^*)$  is computed in M2, it will be reused in M3. The computation of the reduced transfer function  $H_r(s^*)$  costs even less, because  $V$  usually has very few columns. This means that only little additional computation is necessary in order to check the error of the reduced model. Finally, the gain of the proposed adaptive scheme over the standard method PRIMA is that one can determine the order of the reduced model automatically and the accuracy of the reduced model can be adjusted on the fly. Guessing and trial-and-error is thereby completely avoided.

An error indicator proposed in [9] controls the number of moments matched for a given expansion point. It considers the error between the neighboring reduced transfer functions  $e(s_i) = H_r(s_i) - H_{r+1}(s_i)$ ,  $i = 1, 2, \dots, m$ , at many samples of the frequency. This means that the error is derived by computing the two reduced transfer functions whilst sweeping over the whole frequency range. The error is computed at each iteration of adding one moment vector to the Krylov subspace of  $V$ , which needs much more computation than the scheme of error check above. Moreover, a small  $e(s_i)$  cannot guarantee a small  $\varepsilon(s_i)$  in theory. The error control in [6] is based on a similar idea. The proposed scheme computes the real error of the reduced model and therefore guarantees convergence. Moreover, the method in [9] is actually not a fully automatic method, because the expansion points are not chosen automatically.

### 3.2 Adaptive scheme for choosing expansion points, moments and the order

In the following, the adaptive scheme of both choosing expansion points and deciding the number of moments is delineated. Generally speaking, the expansion points are chosen based on a bisection principle. The number of moments matched at each expansion point is determined by a tested point which is known to cause the largest error in the interval of each pair of neighboring expansion points.

#### Adaptive scheme for choosing expansion points, moments and the order $r$ :

E1: At the start one should choose an acceptable dimension of the reduced model, say  $r_{max}$ , as well as the acceptable accuracy of the reduced model  $tol$ .  $r_{max}$  will be adjusted to a proper number during the adaptive scheme if it was selected too small.

E2: The first expansion point is chosen as  $s_0 = s_l$ , the projection matrix  $V$  is computed such that  $\text{range}\{V\} = \text{span}\{\tilde{B}(s_0)\}$ . Compute  $\varepsilon = \|H(s_h) - H_r(s_h)\|/\|H(s_h)\|$ .

E3: Let  $col$  be the number of columns in  $V$ . For  $i = 1, 2, \dots$ , while  $\varepsilon > tol$  and  $col < r_{max}$ , add new moment vectors  $(\tilde{G}(s_0)^{-1}C)^i \tilde{B}(s_0)$  to  $V$ , such that

$$\text{range}\{V\} = \text{span}\{\tilde{B}, \tilde{G}(s_0)^{-1}C\tilde{B}(s_0), \dots, (\tilde{G}(s_0)^{-1}C)^i \tilde{B}(s_0)\}. \text{ Compute } \varepsilon = \|H(s_h) - H_r(s_h)\|/\|H(s_h)\|.$$

E4: Inside the ‘‘For’’ loop in E3, if  $col > r_{max}$ , i.e., if the dimension of the reduced model which will be produced by  $V$  is larger than the acceptable dimension, then add the second expansion point  $s_1 = s_h$  and go to E5. Otherwise, if  $col < r_{max}$  and  $\varepsilon < tol$ , compute the reduced model and stop.

E5: If  $s_1$  is added as the second expansion point, then compute a new matrix  $V$  based on the two expansion points  $s_0 = s_l$  and  $s_1 = s_h$ , such that it includes the 0th order moments  $m_0^{s_l}, m_0^{s_h}$  of both expansion points. I.e.,  $\text{range}\{V\} = \text{span}\{\tilde{B}(s_0), \tilde{B}(s_1)\}$ . Because  $\tilde{B}(s_0)$  has been computed, it is simply picked out from the previously computed matrix  $V$ . One only has to compute  $\tilde{B}(s_1)$ . Now only check the error at  $s_2$ :  $\varepsilon = \|H(s_2) - H_r(s_2)\|/\|H(s_2)\|$ . Here  $s_2 = 2\pi j f_2$  is the midpoint between  $s_0$  and  $s_1$  with  $f_2 = f_0 + (f_1 - f_0)/2$ .

E6: While  $\varepsilon > tol$  and  $col < r_{max}$ , add the  $i$ th ( $i > 0$ ) order moments of both expansion points, such that

$$\begin{aligned} \text{range}\{V\} = \text{span}\{ & \tilde{B}(s_0), \tilde{B}(s_1), \\ & (\tilde{G}(s_0)^{-1}C)\tilde{B}(s_0), (\tilde{G}(s_1)^{-1}C)\tilde{B}(s_1), \\ & \dots, (\tilde{G}(s_0)^{-1}C)^i \tilde{B}(s_0), (\tilde{G}(s_1)^{-1}C)^i \tilde{B}(s_1)\}. \end{aligned} \quad (8)$$

Likewise,  $(\tilde{G}(s_0)^{-1}C)^i \tilde{B}(s_0)$  can be simply picked out from the previous  $V$ , so that only  $(\tilde{G}(s_1)^{-1}C)^i \tilde{B}(s_1)$  is computed.

E7: If  $col > r_{max}$ , then take  $s_2$  as the new expansion point and go to E8. Otherwise, if  $col < r_{max}$  and  $\varepsilon < tol$ , then compute the reduced model and stop.

E8: Compute a new matrix  $V$  based on the above three expansion points, such that it includes the  $i$ th order moments of all expansion points,  $\text{range}\{V\} = \text{span}\{\tilde{B}(s_0), \tilde{B}(s_1), \tilde{B}(s_2)\}$ . Similarly, one only has to compute  $\tilde{B}(s_2)$ , and reuse the other two terms which are computed in the previous steps. Now check the error  $\varepsilon_3 = \|H(s_3) - H_r(s_3)\|/\|H(s_3)\|$  and  $\varepsilon_4 = \|H(s_4) - H_r(s_4)\|/\|H(s_4)\|$ . Likewise,  $s_3$  is the midpoint between  $s_0$  and  $s_2$ , and  $s_4$  is the midpoint between  $s_2$  and  $s_1$ .

E9: While both  $\varepsilon_3 > tol$  and  $\varepsilon_4 > tol$ , and  $col < r_{max}$ , add higher order moments such that

$$\begin{aligned} \text{range}\{V\} = \text{span}\{ & \tilde{B}(s_0), \tilde{B}(s_1), \tilde{B}(s_2), \\ & (\tilde{G}(s_0)^{-1}C)\tilde{B}(s_0), (\tilde{G}(s_1)^{-1}C)\tilde{B}(s_1), \\ & (\tilde{G}(s_2)^{-1}C)\tilde{B}(s_2), \dots, \\ & (\tilde{G}(s_0)^{-1}C)^i \tilde{B}(s_0), (\tilde{G}(s_1)^{-1}C)^i \tilde{B}(s_1), \\ & (\tilde{G}(s_2)^{-1}C)^i \tilde{B}(s_2)\}. \end{aligned}$$

Similarly, one only has to compute the vectors related to  $s_2$ ; the other vectors can be simply picked out from the previous  $V$  and reused. If any of the two cases happens:

- a) Any of the two errors satisfy  $\epsilon_{j_0} < tol$ ,  $j_0 = 3$  or  $4$ , go to E10.
- b)  $col > r_{max}$ , go to E11.

E10: If Case a in E9 and  $col < r_{max}$ , then continue adding the higher order moments of  $s_j$ , which do not lie adjacent to  $s_{j_0}$  and stop adding moments of the two expansion points  $s_i$  which are adjacent to  $s_{j_0}$ , or in other words, which generate  $s_{j_0}$ . For example, if  $j_0 = 3$ , then  $s_i = s_0, s_2$ ,  $s_j = s_1$ . At the same time, stop checking the error at  $s_3$ , and only check the errors at  $s_4$ . If at some stage, the error at  $s_4$  is also smaller than  $tol$  and  $col < r_{max}$ , then stop. Otherwise, only add the current tested midpoint  $s_4$  as the new expansion point.

E11: If Case b in E9, do b, c or d in E13.

E12: Let us consider a general case of  $m$  expansion points. Similarly, the 0th order moments of all expansion points are added to  $V$ , such that  $range\{V\} = span\{\tilde{B}(s_0), \tilde{B}(s_1), \dots, \tilde{B}(s_m)\}$ . For  $i = 1, 2, \dots$ , check each error at the midpoint of each pair of neighboring expansion points. If none of them is smaller than  $tol$ , continue adding the  $i$ th order moments. Otherwise, if any of them, say  $s_{j_0}$  is smaller than  $tol$ , stop adding higher order moments of the two expansion points which generate  $s_{j_0}$ . Also stop checking the error corresponding to  $s_{j_0}$  and only check the midpoints with errors larger than  $tol$ . Keep adding higher moments of corresponding expansion points, until all the left errors are smaller than  $tol$  or  $col > r_{max}$ . Midpoints like  $s_{j_0}$  may arise at different steps of  $i$ , they will be deleted gradually with increasing order  $i$ .

- E13:
- a) If all of the errors are smaller than  $tol$  and  $col < r_{max}$ , then stop. The projection matrix  $V$  of the reduced model is obtained.
  - b) If all of the errors are smaller than  $tol$  and  $col > r_{max}$ , and only the 0th order moments are included in  $range(V)$ , then it means that it is impossible to obtain a reduced model with order smaller than  $r_{max}$  and satisfying the required  $tol$ . The smallest order of the reduced model is  $col$ .
  - c) If not all of the errors are smaller than  $tol$  and  $col > r_{max}$ , and if only the 0th order moments are included in  $range(V)$ , then it means that the initially given  $r_{max}$  is too small to obtain a reduced model satisfying the required  $tol$  and  $r_{max}$ . One should modify the initial  $r_{max}$  to a larger value, e.g.  $r_{max} = 2 * col$ , which is double the number of columns in the current projection matrix  $V$ , and one should add the current left midpoints (except for those deleted points  $s_{j_0}$  with error smaller than  $tol$ ) as the new expansion points, and then repeat E12.
  - d) If not all of the errors are smaller than  $tol$  and  $col > r_{max}$ , and if higher order moments are also included in the current  $range(V)$ , then it tells us that we still have the opportunity to use more expansion points to reduce the order of the reduced model and meet the accuracy requirement  $tol$ . For this case, we do not have to modify  $r_{max}$  and simply need to add the current left midpoints (except for those deleted points  $s_{j_0}$  with error smaller than  $tol$ ) as the new expansion points.

**Explanation for E4:**  $col > r_{max}$  means that there are too many columns in  $V$  for the current single expansion point. It implies that additional expansion points should be added in order to match the frequencies far away from the current expansion point and simultaneously maintain the reduced model at a small size. The next expansion point is taken as the point farthest away from the current expansion point within the specified frequency range.

For the general case in E12, when choosing the expansion points and the moments, the original transfer function needs only to be computed at the  $m - 1$  tested midpoints. The number  $m$  is usually less than 10 when the reduced model satisfies the required  $tol$  and  $r_{max}$ . Therefore, the total extra computation generated by the adaptive scheme is still small.

**Explanation for E5:** Because  $s_2$  is the point which is farthest away from both  $s_0$  and  $s_1$ , we assume that the point which causes the largest error is usually around  $s_2$ . Therefore, we only test the error at  $s_2$  and expect that if the error at  $s_2$  is smaller than  $tol$ , then the errors at all other points will also be smaller than  $tol$ , or at least close to the error at  $s_2$ . Similarly in E12, it is sufficient to check the errors only at the tested midpoints, because they are the points which are farthest away from the current expansion points. In fact, there are special cases for which the error at  $s_2$  is much smaller than the errors at other points between  $s_0$  and  $s_1$ . The same may also happen to other midpoints in E8 and E12, e.g. at  $s_3$  and  $s_4$ . We will deal with these cases in the next subsection.

The motivation of our approach regarding the adaptive selection of expansion points in some sense resembles the greedy sampling procedures used in reduced basis (RB) methods for the model reduction of parameterized partial differential equations, see, e.g. [10], [11] and references therein. In [10, 11], the points which cause the locally largest error (rather than the global largest error considered in our method) are selected as the candidates for the expansion points. The selection process is done by local optimization. The whole process is much more complex than our method and requires much more computation, because the original system has to be repeatedly simulated. A direct comparison of the algorithms is difficult as greedy sampling is usually performed in parameter space, while our expansion points are taken with respect to frequencies. A further exploration of similarities and differences is beyond the scope of this paper and will be the topic of further research. It should also be noted that our adaptive moment selection process has no direct analogy in greedy sampling/RB methods.

#### **Adaptively finding the order of the reduced model**

It can be seen from step E13 that the order of the reduced model can also be adaptively determined if the initially given  $r_{max}$  is too small to obtain a sufficiently accurate reduced model. For example, if  $r_{max}$  is set to be 10, and the reduced model is still not accurate enough, then we can set a larger  $r_{max}$ , and continue adding more expansion points to obtain a new reduced model. The previously computed moments vectors can still be made use of, and the algorithm does not have to be restarted. After a few iterations, a new reduced model with an adaptively determined order is obtained.

### **3.3 Modification scheme for the tested midpoints**

The above special cases in E5 happen if the two expansion points  $s_0, s_1$  separately cause very different errors at  $s_2$ . This means that if we compute two individual reduced transfer functions  $H_{r_0}$  and  $H_{r_1}$  by expanding the original transfer function  $H(s)$  at  $s_0$  and  $s_1$ , re-

spectively, and by matching the same number of moments, the error of  $H_{r_0}$  at  $s_2$ ,  $\varepsilon_0(s_2) = \|H(s_2) - H_{r_0}(s_2)\|/\|H(s_2)\|$  is either much smaller or much larger than the error of  $H_{r_1}$  at  $s_2$ ,  $\varepsilon_1(s_2) = \|H(s_2) - H_{r_1}(s_2)\|/\|H(s_2)\|$ . For example, it could happen that  $\varepsilon_0(s_2) = 1$ ,  $\varepsilon_1(s_2) = 1e - 5$ . In this case, if we derive a single reduced transfer function by using multi-point expansion for  $H(s)$ , i.e., expanding  $H(s)$  at  $s_0$  and  $s_1$ , the error  $\varepsilon^*(s_2)$  of the single reduced transfer function at  $s_2$  could also turn out to be much smaller than  $\varepsilon_0(s_2)$ . This is because  $s_1$  contributes more to the accuracy of the reduced model at  $s_2$  than  $s_0$  does, therefore speeds up the decrease of  $\varepsilon^*(s_2)$ . If we continue matching more moments at  $s_0$  and  $s_1$  and checking  $\varepsilon^*(s_2)$ , then it probably becomes smaller than  $tol$  more quickly than would the errors at other points which are closer to  $s_0$ . This is because those points are farther away from  $s_1$ , so that  $s_1$  could not contribute as much as  $s_2$ . As a result, the algorithm stops before the error of the reduced model is smaller than  $tol$  at all the frequencies.

One solution to the above problem is to modify the current tested midpoint  $s_2$  to a new point  $s^*$  such that  $s^*$  satisfies  $min < \varepsilon_0(s^*)/\varepsilon_1(s^*) < max$ . Here  $max$ ,  $min$  are taken as some reasonable values, which show that the difference between  $\varepsilon_0(s^*)$  and  $\varepsilon_1(s^*)$  should not be too big. One can take e.g.  $max = 10$ ,  $min = 0.1$ . In order to find  $s^*$ , we take a few samples between  $s_0$  and  $s_2$  if  $\varepsilon_0(s_2) > \varepsilon_1(s_2)$ , otherwise, we take a few samples between  $s_2$  and  $s_1$ . We compare  $\varepsilon_0$  and  $\varepsilon_1$  at the samples one after the other until  $s^*$  is found. During the process, the values of the original transfer function  $H(s)$  at the sample points have to be estimated. However, the samples are usually very few and less than 10. Furthermore, it is not necessary that  $H(s)$  be computed at all the sample points; usually  $s^*$  has been found before all the sample points are estimated. Therefore, the computational complexity of finding  $s^*$  is equivalent to matching a few more moments.

If we look at  $min < \varepsilon_0(s^*)/\varepsilon_1(s^*) < max$ , it tells us that the difference between  $H_{r_0}(s^*)$  and  $H_{r_1}(s^*)$  should not be large. Therefore we can also use the criterion  $min < \|H_{r_0}(s^*)\|/\|H_{r_1}(s^*)\| < max$  as the stopping criterion of searching  $s^*$ . In this way, we avoid calculating the original transfer function at the sample points, which will save computation time.

Our modification scheme applies to any tested midpoint between any pair of neighboring expansion points. This means that if the above case happens to other expansion points other than  $s_0, s_1$ , we can treat those tested midpoints in the same way.

Note that, for the case that any midpoint  $s_{mid}$  is modified to a new tested point  $s^*$ ,  $s^*$  rather than  $s_{mid}$  will be selected as the new expansion point in E13. In this way, we have realized the fully adaptive scheme, which only checks the errors of the points which really produce the largest errors. The resulting expansion points may not be located equidistantly between  $s_l$  and  $s_h$ , a situation which is best explained by Table 9 in Section 4.

### 3.4 Illustration of the adaptive scheme with diagrams

To render the above scheme clearer, we plot a flowchart of the general steps of the scheme in Fig 1. At step 2 in the flowchart,  $s_1, \dots, s_m$  represent the current expansion points including the newly added expansion points. We check if the error of the reduced transfer function  $H_r(s)$  at all of the tested points is smaller than  $tol$  at step 3. If true, we proceed to step 4.1, otherwise we go to step 4.2. At step 4.2 we further check whether the error of  $H_r(s)$  is smaller than  $tol$  at some of the tested points in order to remove those expansion points which already have satisfied the error tolerance from the current expansion point list. In the next step, only those

expansion points having unacceptable error have to be matched with higher order moments. During step 3 and step 4.2, we use the modification scheme in Subsection 3.3 to modify the tested mid-points if necessary.

At step 4.1, if  $r > r_{max}$ , we further check at step 5.1, and see if it is at the initial stage of moment matching, i.e., whether only the 0th order moments ( $i = 0$ ) are included in the Krylov subspace. If true, this means the current  $r_{max}$  is too small. The proper order of the reduced model is the current  $r$ . If  $i > 0$ , then we can directly add new expansion points and proceed to step 2. We have similar checks at steps 6.1 and 6.2.

In the flowchart, the new expansion points are those tested points (either the midpoints or the modified points) at which the error of the reduced transfer function  $H_r(s)$  is still larger than  $tol$ .

The technique of adding the expansion points is illustrated in Fig 2. Iteration  $i$ ,  $i = 0, 1, \dots$ , describes the stage where  $s_0, \dots, s_{2^i}$  are in the set current expansion points. In Fig 3, we plot the error of the reduced transfer function  $H_r(s)$  versus the number of expansion points. The error of  $H_r(s)$  should decrease with increasing number of expansion points. For the current iteration  $i$ , with  $s_0, \dots, s_{2^i}$ ,  $i = 0, 1, \dots$  representing the expansion points, the error of  $H_r(s)$  is measured only at the tested points between each pair of the neighboring expansion points, which are also marked in the figure.

From the above analysis, we see that the scheme is reasonable and operative w.r.t. theoretical and numerical aspects. In the next section, we demonstrate the robustness of our adaptive scheme using several examples. For some of them, the standard moment-matching method PRIMA behaves badly. Our adaptive scheme produces reduced models with the desired reduced order and accuracy. In all cases, the expansion points, the number of moments matched and the order  $r$  are determined automatically.

## 4 Simulation results

### 4.1 The examples

In this section, we use several examples to test the efficiency of the adaptive scheme. The first example is an RLC tree circuit, which can be instantiated for any level  $l$ . Between two consecutive levels, the circuit branch segments of the lower level each split into two children, yielding  $\sum_{i=0}^{l-1} 2^i$  in the circuit of level  $l$ . Each segment is made up of four RL pairs in series, representing the wiring on a chip, with four capacitors to ground, representing the wire-substrate interaction, see Fig. 4. We construct two models for the example with respect to different levels of  $l$ . The dimension of the two models are  $n = 6134$  and  $n = 24566$  respectively.

The second example, shown in Fig. 5, is a three conductor radio-frequency busline model, split into 16 RLC segments. The two outer busline conductors of the coplanar waveguide are terminated at both ends with resistors to ground. The middle signal line is terminated by a capacitor to ground at the one end, and is driven at the other end by a current source shunted by a resistor to ground. The segment model represents each conductor segment by a line resistance, an inter-segment capacitance, a line self-conductance, and an inter-segment mutual inductance. The original system is of size  $n = 147$ . For both examples, the input for

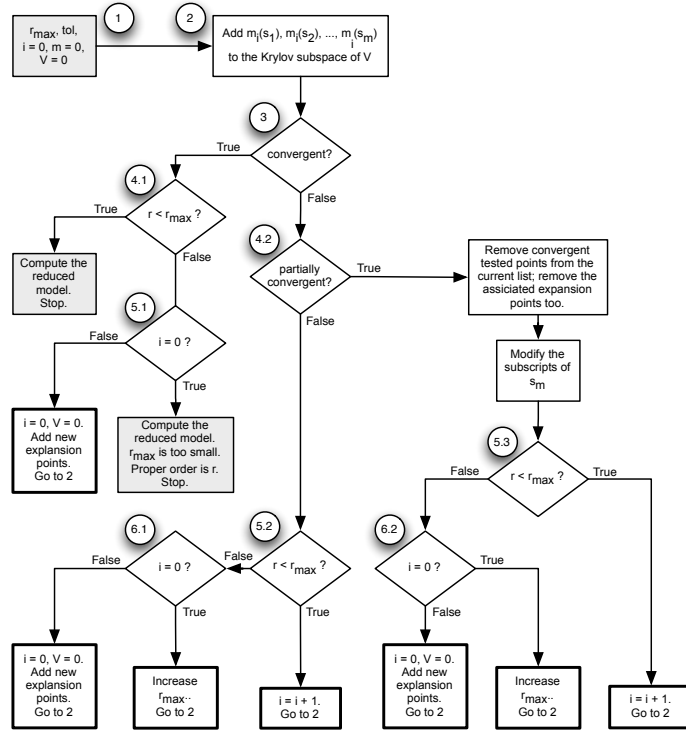


Figure 1: Flowchart of the scheme.

each example is a step signal with 0.1 ns rise time, and the frequency range of interest is set as  $[f_l, f_h] = [0, 3 \text{ GHz}]$  [5].

The third example results from a PEEC discretization of an on-chip metallic spiral inductor in a square geometry. The inductor features a ground plane shield that extends beyond the inductor's outer windings. In addition, the inductor features a grounded guard ring which helps to reduce parasitics even further, see Fig. 6<sup>1</sup>. This example has been tested by many methods, including those based on balanced truncation [12]. The resulting descriptor system is of dimension  $n = 1434$ . The interesting parameter for this example is the resistance and inductance of the inductor and the frequency range of interest is  $[f_l, f_h] = [0, 10 \text{ GHz}]$ .

All of the above three examples are single input and single output (SISO) systems. For the fourth example, we provide simulation results for a multiple input and multiple output (MIMO) system. The model is obtained from the SLICOT benchmark collection <sup>2</sup>. It is derived from an electrical circuit of a CMOS-inverter driven two-bit bus modelled by 40 RLC

<sup>1</sup>The details of this example can be found at URL: [http://simulation.uni-freiburg.de/downloads/benchmark/Peek-inductor\(38891\)](http://simulation.uni-freiburg.de/downloads/benchmark/Peek-inductor(38891))

<sup>2</sup>(URL: <http://www.icm.tu-bs.de/NICONET/benchmodred.html>)

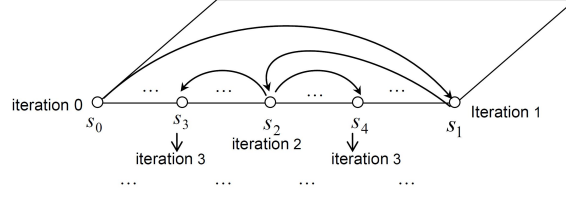


Figure 2: Bisection principle of choosing expansion points.

sections whose discretized equation system was determined using modified modal analysis available in Spice, yielding a numerical system with order  $n = 980$ , and which has 4 inputs and 4 outputs [7]. The frequency of interest is  $[f_l, f_h] = [0, 3 \text{ GHz}]$ :

## 4.2 Rules of implementation

We set  $r_{max} = 20$  for the SISO models, and set  $r_{max} = 50$  for the MIMO model. For the SISO examples, the relative error  $e_R$  between the reduced transfer function and the original transfer function is measured by  $e_R = \max_{s_i} |H(s_i) - H_r(s_i)| / |H(s_i)|$ , where we have taken 2000 frequency samples  $s_i = 2\pi j f_i$ ,  $i = 1, 2, \dots, 2000$ . For the MIMO example, we use  $e_R^{ik}$  instead of  $e_R$  to indicate the relative error of the  $(i, k)$ th entry of the reduced transfer matrix  $H_r(s)$ . We use  $H_{ik}(s)$  to represent the  $(i, k)$ th entry of  $H(s)$  and  $H_{r_{ik}}(s)$  to represent the  $(i, k)$ th entry of  $H_r(s)$ .  $H_{ik}(s)$  is the transfer function relating the  $i$ th input to the  $k$ th output. We define  $e_R^{ik} = \max_{s_i} |H_{ik}(s_i) - H_{r_{ik}}(s_i)| / |H_{ik}(s_i)|$ ,  $i = 1, 2, \dots, 2000$ . Here,  $|\cdot|$  means the magnitude of the transfer function.

For all but the spiral inductor example, the frequency range of interest is  $[0, 3 \text{ GHz}]$ , therefore we have set  $s_l = 0$  and  $s_h = 2\pi j 3 \text{ GHz}$  in the adaptive scheme. For the spiral inductor, we have  $s_h = 2\pi j 10 \text{ GHz}$ . All of the simulation results are obtained with MATLAB® version 2007b.

For the adaptive scheme for the SISO models, the error in the adaptive scheme  $\varepsilon(s^0) = ||H(s^0) - H_r(s^0)|| / ||H(s^0)||$  at a certain point  $s^0$  is defined as  $\varepsilon(s^0) = |H(s^0) - H_r(s^0)| / |H_r(s^0)|$ . I.e. this is the relative error of the reduced transfer function at  $s^0$ . When applying the adaptive scheme to the MIMO example, the error  $\varepsilon(s^0)$  at a certain point  $s^0$  is computed as  $\varepsilon(s^0) = \max_{ik} |H_{ik}(s^0) - H_{r_{ik}}(s^0)| / |H_{ik}(s^0)|$ , which is the maximal relative error of the entries  $H_{r_{ik}}$  at  $s^0$ . It can also be explained as the maximal relative error of the reduced transfer functions  $H_{r_{ik}}$  relating the  $i$ th input signal to the  $k$ th output signal,  $i, k = 1, 2, \dots, 4$ .

Once the errors  $\varepsilon(s^i)$  at all of the tested points  $s^i$  are smaller than  $tol$ , the reduced model is obtained.

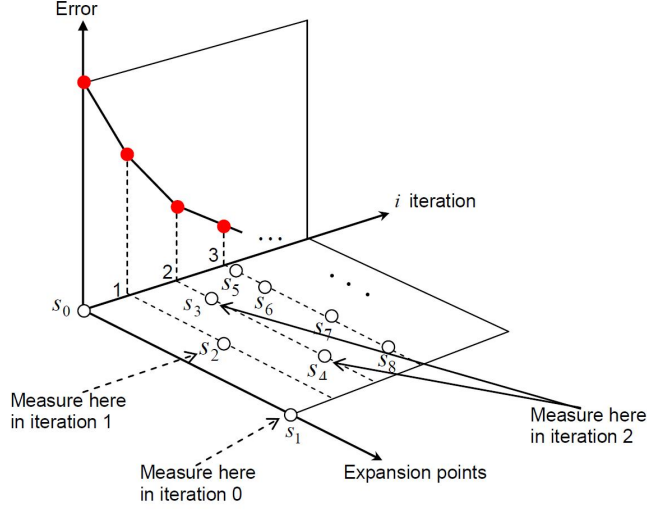


Figure 3: Scheme of error control and change of the error with the number of expansion points.

### 4.3 Results of the adaptive scheme for a fixed $tol$

In this section, we show the results of the adaptive scheme when  $tol = 1 \times 10^{-2}$  for all the examples.

#### 4.3.1 Results for the SISO examples

For the model of the clock tree with  $n = 24566$ , the expansion points are adaptively chosen as  $s_0 = s_l = 2\pi j f_0 = 0$ ,  $s_1 = s_h = 2\pi j f_h = 2\pi j 3$  GHz, and  $s_2 = s_l + (s_h - s_l)/2$ , the midpoint of  $s_l$  and  $s_h$ . Here  $f_0 = 0$ ,  $f_h = 3$  GHz are the corresponding frequency points. The moments matched at each expansion point is  $q = 4$ . The order of the reduced model is  $r = 20$ . The relative error  $e_R$  of the reduced transfer function is plotted in Fig. 7. According to our adaptive scheme, the tested point for error control is the midpoint  $s_3$  between  $s_l$  and  $s_2$  and the midpoint  $s_4$  between  $s_2$  and  $s_h$ . From the figure, we see the frequency points with the largest errors are very close to  $f_3 = 1.5$  GHz and  $f_4 = 2.25$  GHz ( $s_i = 2\pi j f_i$ ,  $i = 3, 4$ ), which is in agreement with our adaptive scheme.  $f_4$  is also the final tested midpoint which produces the largest error. The other midpoint  $f_3$  corresponds to  $s_{j_0}$  in E10, and it is removed from the list of midpoints during the adaptive scheme.

For the model of the clock tree with  $n = 6134$ , two expansion points have been adaptively chosen,  $s_0 = s_l = 0$ ,  $s_1 = s_h$ . The number of moments matched at each expansion point is  $q = 6$ . The reduced model is of order  $r = 18$ . Fig. 8 gives the relative error of the reduced transfer function. It shows that the error around the midpoint between  $s_l$  and  $s_h$  is the largest; this further justifies our adaptive scheme. From Fig. 9, we see that the reduced transfer function matches the original transfer function very well for each peak. The error of the reduced transfer

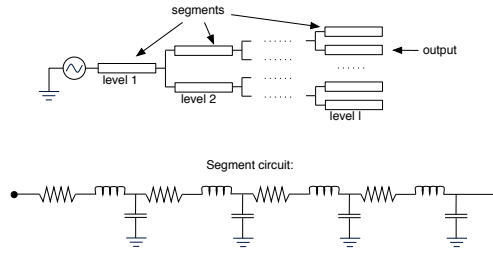


Figure 4: A clock tree example.

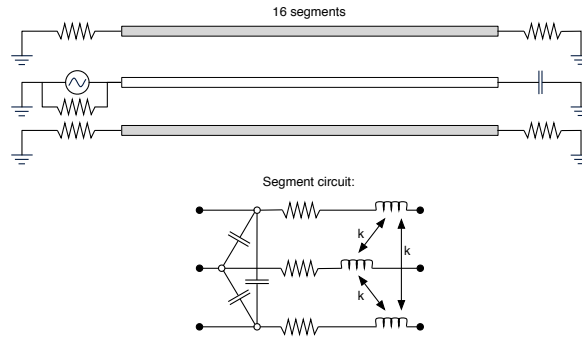


Figure 5: A busline example.

function of the clock tree model with  $n = 24566$  ( $e_R$  in Fig. 7) is even smaller than  $e_R$  in Fig. 8, therefore, the reduced transfer function of the model with  $n = 24566$  should match the original transfer function even better. To avoid repetition, we do not show it here.

We obtain a reduced model of order  $r = 3$  for the busline model. For this example, only  $s_0 = s_l$  is used for expansion and  $q = 3$  moments are matched. The tested point for error control is  $s_h = 2\pi j3$  GHz. The error of the reduced transfer function is plotted in Fig. 10. As we can see, the error at  $f^* = 3$  GHz is the largest.

The relative error  $e_R$  of the reduced transfer function of the spiral inductor model is plotted in Fig. 11, which remains below  $tol = 10^{-2}$  for all frequencies. It shows that the error at  $f^* = 10$  GHz is the largest, which corresponds to the tested point  $s_h$ . The reduced system is of order  $r = 9$  and only  $s_0 = s_l$  is used as the expansion point; the tested point picked by the adaptive scheme is  $s_h$ .

Fig. 12 includes the resistance of the spiral inductor obtained by full simulation of the original system as well as the resistance computed from the reduced system. Fig. 13 compares the inductances of the spiral inductor computed respectively from the original system and the reduced system. Unfortunately, the reduced model produces an inaccurate resistance whose

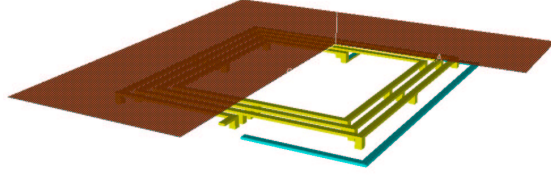


Figure 6: Spiral inductor with part of overhanging copper plane.

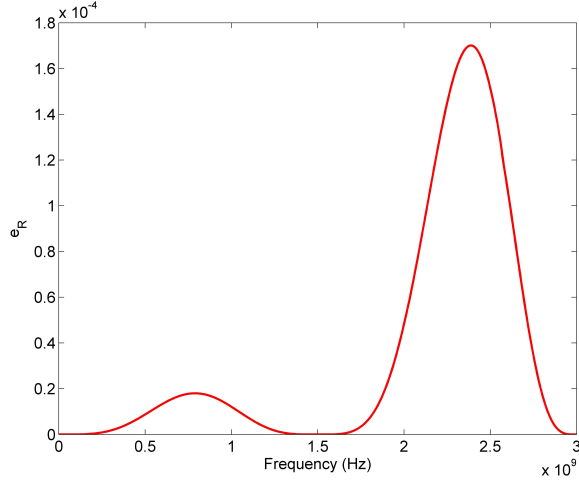


Figure 7: Error of the reduced transfer function of the clock tree model with  $n = 24566$ .

error is larger than  $tol = 1 \times 10^{-2}$ . This may be because the resistance is reciprocally related to the real part of the transfer function. If we set  $tol = 1 \times 10^{-3}$ , we see that the resistance (the star symbol line in Fig. 13) is already indistinguishable from the full simulation result. With  $tol = 1 \times 10^{-3}$ , the reduced model is of order  $r = 9$ , but has used two expansion points instead.

#### 4.3.2 Results of the MIMO example

We compare  $H_{ik}$  with  $H_{r_{ik}}$  for each pair of  $ik$ ,  $i, k = 1, 2, \dots, 4$  and list the relative error  $e_R^{ik}$  between  $H_{ik}$  and  $H_{r_{ik}}$  in Table 1. The order of the reduced model is  $r = 48$ . Two expansion points  $s_0 = s_l = 0$ ,  $s_1 = s_h = 2\pi j f_h = 2\pi j 3$  GHz have been used, and 4 moments are matched for each expansion point. The tested point is the midpoint  $s_2 = s_0 + (s_0 - s_1)/2$ . We see from Table 1 that the error of the reduced transfer function  $H_{r_{ik}}$ ,  $i, k = 1, 2, \dots, 4$  in the whole frequency interval is very close to  $tol$ , though not below  $tol$ .

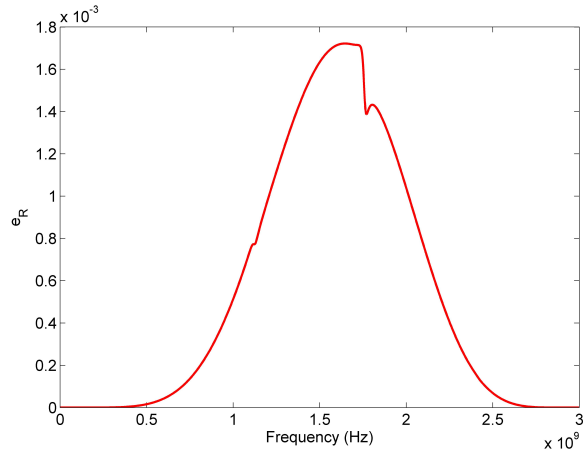


Figure 8: Error of the reduced transfer function of the clock tree model with  $n = 6134$ .

Table 1:  $e_R^{ik}$  for each pair  $ik$  for the MIMO example with  $tol = 1 \times 10^{-2}$  and  $r_{max} = 50$

$e_R^{ik}$	pair 11	pair 12	pair 13	pair 14
	$2.98 \times 10^{-2}$	$1.22 \times 10^{-2}$	$1.38 \times 10^{-2}$	$3.1 \times 10^{-2}$
$e_R^{ik}$	pair 21	pair 22	pair 23	pair 24
	$1.22 \times 10^{-2}$	$2.96 \times 10^{-2}$	$3.09 \times 10^{-2}$	$1.38 \times 10^{-2}$
$e_R^{ik}$	pair 31	pair 32	pair 33	pair 34
	$1.38 \times 10^{-2}$	$3.09 \times 10^{-2}$	$3.23 \times 10^{-2}$	$1.12 \times 10^{-2}$
$e_R^{ik}$	pair 41	pair 42	pair 43	pair 44
	$3.1 \times 10^{-2}$	$1.38 \times 10^{-2}$	$1.12 \times 10^{-2}$	$3.15 \times 10^{-2}$

It is worth mentioning that, if we run PRIMA with the above indicated expansion points and number of moments, then the computed reduced model produces almost the same results as that produced by our adaptive scheme.

#### 4.4 Efficiency of the modification scheme

In this subsection, we demonstrate the efficiency of the modification scheme proposed in Subsection 3.3 to find the smallest sufficiently accurate system. We take the spiral inductor as an example for explanation. More simulation results to which the modification scheme has been applied can be found in Table 4, Table 6, Table 9 and Table 10 in Subsection 4.5.

From Subsection 4.3, we know that if  $tol = 1 \times 10^{-2}$ , we cannot obtain a reduced model which gives the correct resistance of the spiral inductor within acceptable accuracy. We need to set  $tol = 1 \times 10^{-3}$ , where two expansion points  $s_0 = s_l$  and  $s_1 = s_h$  are adaptively chosen. If

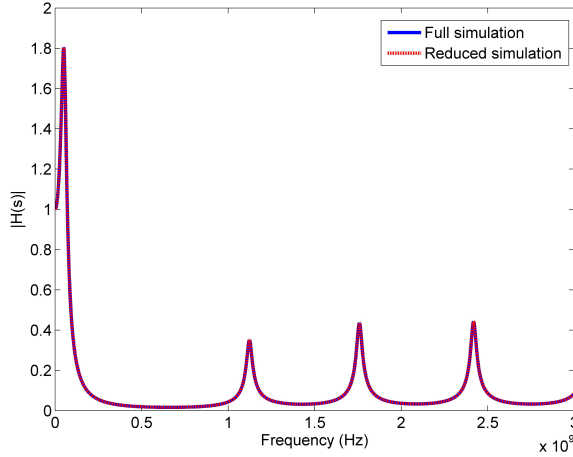


Figure 9: Comparison of the transfer functions of the clock tree model with  $n = 6134$ .

we do not use the modification scheme in Subsection 3.3, the tested point for the error control is the midpoint  $s_2 = 2\pi j f_2$  with  $f_2 = 5 \times 10^9$  between  $s_l$  and  $s_h$ . The reduced model is of order  $r = 6$ . The error of the transfer function is plotted in Fig. 14 (solid line). We see that the error is largest at the frequency around  $f = 1 \times 10^8$  rather than the midpoint  $f_2$ . And the error of the reduced transfer function is actually not smaller than  $tol = 1 \times 10^{-3}$  at all frequencies, though the error at  $s_2$  is already around  $10^{-6}$ . As is analyzed in Subsection 3.3, this is because the errors of the individual reduced transfer functions computed respectively by  $s_l$  and  $s_h$  at  $s_2$  show a large difference. For this example, when  $q = 1$ , we have that  $\varepsilon_0(s_2)/\varepsilon_1(s_2) = 5 \times 10^3$ .

However if we use the modification scheme of Subsection 3.3, and set  $max = 10$ ,  $min = 0.1$ , a new tested point  $s^* = 2\pi j f^*$ ,  $f^* = 1.58 \times 10^8$  is found. Using this new tested point, the reduced model we obtain is of order  $r = 9$ .  $q = 3$  moments have been matched for each expansion point. The error plot of the reduced transfer function is the line with stars in Fig. 14. The frequency point with the largest error is around  $f = 1 \times 10^8$ , which agrees with the result of our modification scheme and is very close to the new tested frequency point  $f^*$ .

#### 4.5 Adaptivity to different $tol$

In some applications, the above assigned acceptable error  $tol = 10^{-2}$  for the reduced models maybe insufficient, and one may need more accurate models. In order to show the adaptivity of the scheme to different requirements for the accuracy of the reduced models, we list in the following tables the data of the reduced models derived by the adaptive scheme for different  $tol$ , and for different examples. For the SISO examples, we list  $e_R$  in the table. For the MIMO example, we only list the maximal error  $e_R^{max}$ , the minimal error  $e_R^{min}$  among  $e_R^{ik}$ ,  $i, k = 1, 2, \dots, 4$ , as well as the average error  $e_R^{ave}$ . I.e.  $e_R^{max} = \max_{ik} e_R^{ik}$ ,  $e_R^{min} = \min_{ik} e_R^{ik}$ ,  $e_R^{ave} = (\sum_{ik} e_R^{ik})/16$ .

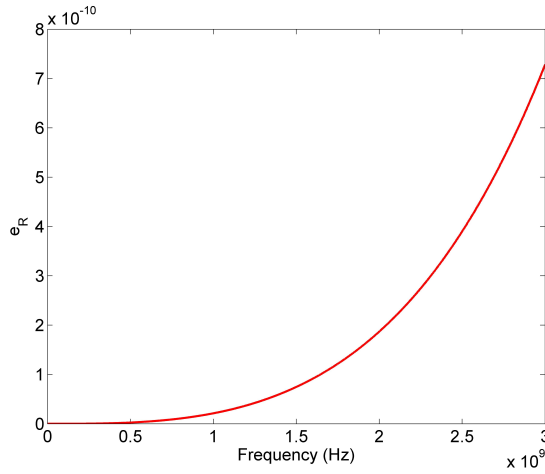


Figure 10: Error of the reduced transfer function of the busline model.

For each model, we set an initial  $r_{max}$ , and the reduced models are derived by requiring that  $r \leq r_{max}$ . If the initially set  $r_{max}$  is too small (see Step E13 in the adaptive scheme), then a reduced model with order larger than  $r_{max}$  could be obtained.

From Table 2, we see that almost all of the reduced models meet the requirements of  $tol$ . There are exceptional cases for the spiral inductor example. This is reasonable, because the tested point between each two neighboring expansion points chosen by the adaptive scheme sometimes is not exactly the point (e.g.  $s'$ ) with the largest error. In such cases, if the tested point  $s^T$  is not close enough to  $s'$ , the error of  $H_r$  at  $s'$  could have a relatively large difference from  $H_r(s)$  at  $s^T$ . As a result, the error of  $H_r(s')$  maybe still a bit larger than  $tol$ , although the error of  $H_r(s^T)$  is already below  $tol$ .

However, the accuracy of the reduced model can be further improved at least for one possible cause of the exceptional cases. If the inaccuracy of such cases is caused by the large range  $[\min, \max]$  assigned for  $\epsilon_0(s^*)/\epsilon_1(s^*)$  in Subsection 3.3, then by using a smaller range, we have a more accurate estimation of the tested point  $s^T$  which could be even closer to  $s'$ . All of the results in Table 2 are derived by using  $max = 10$  and  $min = 0.1$ . However, when we use tighter values, e.g.  $max = 2$  and  $min = 0.5$ , we can obtain more accurate reduced models. Taking the spiral inductor as an example, the reduced model actually does not satisfy the accuracy  $tol = 1 \times 10^{-3}$  in Table 2, and the reduced transfer function has an error which is slightly larger than  $tol$ . If we use  $max = 2$  and  $min = 0.5$  to recompute the reduced model, the newly obtained reduced model is of order  $r = 12$  and has an error =  $4.2634 \times 10^{-5}$  which is smaller than  $tol = 1 \times 10^{-3}$ . We have used the same 2 expansion points, but the tested point has been modified from  $s^* = 2\pi j f^* = 2\pi j 1.58 \times 10^8$  to  $s^* = 2\pi j f^* = 2\pi j 9.98 \times 10^7$ . The new tested point is that one which causes almost the largest error, because the error of  $H_r(s)$  at the new  $s^*$  is now  $H(s^*) = 4.0015 \times 10^{-5}$  and the largest error of  $H(s)$  at 2000 frequency

Table 2: Adaptivity of the Scheme for Different  $tol$ 

Examples	$r_{max}$	order $r$	$tol$	$e_R/e_R^{max}$
Clock tree n=24566	20	20	$1 \times 10^{-2}$	$1.7008 \times 10^{-4}$
		20	$1 \times 10^{-3}$	$1.7008 \times 10^{-4}$
		22	$1 \times 10^{-4}$	$2.1241 \times 10^{-6}$
		22	$1 \times 10^{-5}$	$5.9384 \times 10^{-6}$
		23	$1 \times 10^{-6}$	$9.9152 \times 10^{-7}$
		29	$1 \times 10^{-7}$	$5.4301 \times 10^{-10}$
		29	$1 \times 10^{-8}$	$3.4221 \times 10^{-10}$
Clock tree n=6134	20	18	$1 \times 10^{-2}$	$1.7 \times 10^{-3}$
		19	$1 \times 10^{-3}$	$3.9734 \times 10^{-5}$
		19	$1 \times 10^{-4}$	$3.9734 \times 10^{-5}$
		18	$1 \times 10^{-5}$	$8.9108 \times 10^{-6}$
		22	$1 \times 10^{-6}$	$8.4101 \times 10^{-7}$
		25	$1 \times 10^{-7}$	$6.7093 \times 10^{-9}$
		29	$1 \times 10^{-8}$	$1.1163 \times 10^{-10}$
Bus line n=147	20	3	$1 \times 10^{-2}$	$7.2863 \times 10^{-10}$
			$1 \times 10^{-3}$	
			$1 \times 10^{-4}$	
			$1 \times 10^{-5}$	
			$1 \times 10^{-6}$	
			$1 \times 10^{-7}$	
			$1 \times 10^{-8}$	
Spiral inductor n=1434	20	9	$1 \times 10^{-2}$	$7.9 \times 10^{-3}$
		9	$1 \times 10^{-3}$	$1.5 \times 10^{-3}$
		12	$1 \times 10^{-4}$	$4.2634 \times 10^{-5}$
		15	$1 \times 10^{-5}$	$8.2020 \times 10^{-6}$
		18	$1 \times 10^{-6}$	$1.1274 \times 10^{-6}$
		16	$1 \times 10^{-7}$	$2.1676 \times 10^{-8}$
		20	$1 \times 10^{-8}$	$1.2086 \times 10^{-9}$

Table 3: Adaptivity of the Scheme for Different  $tol$ , MIMO example  $n = 980$  with  $r_{max} = 50$ 

order $r$	$tol$	$e_R^{min}$	$e_R^{max}$	$e_R^{ave}$
48	$1 \times 10^{-3}$	$1.12 \times 10^{-2}$	$3.23 \times 10^{-2}$	$2.18 \times 10^{-2}$
	$1 \times 10^{-4}$			
54	$1 \times 10^{-5}$	$1.6826 \times 10^{-7}$	$2.2487 \times 10^{-6}$	$8.4729 \times 10^{-7}$
48	$1 \times 10^{-6}$	$9.3259 \times 10^{-5}$	$2.4389 \times 10^{-4}$	$1.8422 \times 10^{-4}$
55	$1 \times 10^{-7}$	$5.7158 \times 10^{-7}$	$2.7846 \times 10^{-6}$	$1.4014 \times 10^{-6}$
61	$1 \times 10^{-8}$	$1.6792 \times 10^{-7}$	$2.2456 \times 10^{-6}$	$8.2128 \times 10^{-7}$

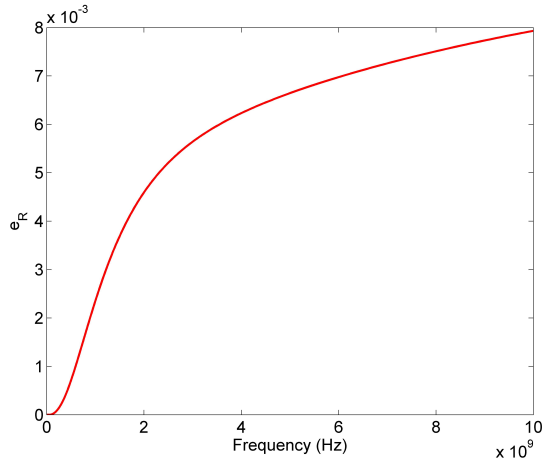


Figure 11: Error of the reduced transfer function of the spiral inductor.

samples  $s_i = 2\pi j f_i$ ,  $i = 1, 2, \dots, 2000$  is  $\max_{s_i} e_R = 4.2634 \times 10^{-5}$ . The two errors are of course very close. Therefore, with the modified *max*, and *min*, we can test for the point which causes the largest error even more accurately. The accuracy of the reduced model corresponding to  $tol = 1 \times 10^{-6}$  can also be improved by using the same technique.

Unfortunately, the accuracy of the reduced models for the MIMO example in Table 3 cannot be improved any more even if the new *max* = 2 and *min* = 0.5 is used. This means that the inaccuracy of the reduced model is not due to the large range [min, max]. A more efficient modification scheme for estimating more accurate tested points for the MIMO systems is therefore still an open problem.

In Table 4-Table 10, we show the expansion points used, and the moments matched for each expansion point according to different *tol* for each example. To obtain a clearer view, we show the frequency points  $f_i$  corresponding to each expansion point  $s_i = 2\pi j f_i$ ,  $i = 1, 2, \dots$  instead of  $s_i$ . As we can see, in some cases the expansion points are not equidistantly distributed. The moments matched are not equal from one point to the next either. Especially from Table 9, we can easily see the expansion points are also not the direct result of using the bisection principle. This is because the modification scheme in Subsection 3.3 has been used during model reduction, where the mid tested points may have been modified to other tested points which are again the candidates for the new expansion points if the error of the reduced model is not small enough. One can imagine how often model reduction would need to be repeated (with a scheme such as PRIMA) in order to obtain a reduced model satisfying the same accuracy and the same order.

Table 4: Expansion points and moments matched for the clock tree  $n = 6134$

$tol = 1 \times 10^{-3}$		$tol = 1 \times 10^{-4}$	
expansion points	moments	expansion points	moments
0	4	0	4
$1.5000 \times 10^9$	4	$1.5000 \times 10^9$	4
$3.0000 \times 10^9$	4	$3.000 \times 10^9$	4
$tol = 1 \times 10^{-5}$		$tol = 1 \times 10^{-6}$	
expansion points	moments	expansion points	moments
0	1	0	1
$0.3750 \times 10^9$	1	$0.1875 \times 10^9$	1
$0.7500 \times 10^9$	1	$0.3750 \times 10^9$	1
$1.1250 \times 10^9$	1	$0.5625 \times 10^9$	1
$1.5000 \times 10^9$	1	$0.7500 \times 10^9$	1
$1.8750 \times 10^9$	1	$0.9375 \times 10^9$	1
$2.2500 \times 10^9 j$	1	$1.1250 \times 10^9$	1
$2.6250 \times 10^9$	1	$1.3125 \times 10^9$	1
$2.8125 \times 10^9$	1	$1.5000 \times 10^9$	1
$3.0000 \times 10^9$	1	$1.6875 \times 10^9$	1
		$1.8750 \times 10^9$	1
		$2.0625 \times 10^9$	1
		$2.2500 \times 10^9 j$	1
		$2.3438 \times 10^9$	1
		$2.4375 \times 10^9$	1
		$2.5313 \times 10^9$	1
		$2.6250 \times 10^9$	1
		$2.7188 \times 10^9$	1
		$2.8125 \times 10^9$	1
		$2.9062 \times 10^9$	1
		$3.0000 \times 10^9$	1

Table 5: Expansion points and moments matched for the clock tree  $n = 6134$  (continued)

$tol = 1 \times 10^{-7}$		$tol = 1 \times 10^{-8}$	
expansion points	moments	expansion points	moments
0	1	0	1
$0.1875 \times 10^9$	1	$0.1875 \times 10^9$	1
$0.3750 \times 10^9$	1	$0.2813 \times 10^9$	1
$0.5625 \times 10^9$	2	$0.3750 \times 10^9$	1
$0.75 \times 10^9$	1	$0.4687 \times 10^9$	1
$0.9375 \times 10^9$	1	$0.5625 \times 10^9$	1
$1.1250 \times 10^9$	1	$0.6563 \times 10^9$	1
$1.3125 \times 10^9$	1	$0.7500 \times 10^9$	1
$1.5000 \times 10^9$	2	$0.8437 \times 10^9$	1
$1.6875 \times 10^9$	2	$0.9375 \times 10^9$	1
$1.8750 \times 10^9$	1	$1.0312 \times 10^9$	1
$2.0625 \times 10^9$	2	$1.1250 \times 10^9$	1
$2.2500 \times 10^9$	2	$1.2188 \times 10^9$	1
$2.4375 \times 10^9$	2	$1.3125 \times 10^9$	1
$2.6250 \times 10^9$	2	$1.4063 \times 10^9$	1
$2.8125 \times 10^9$	2	$1.5000 \times 10^9$	1
$3.0000 \times 10^9$	2	$1.5938 \times 10^9$	1
		$1.6875 \times 10^9$	1
		$1.7812 \times 10^9$	1
		$1.8750 \times 10^9$	1
		$1.9687 \times 10^9$	1
		$2.0625 \times 10^9$	1
		$2.1563 \times 10^9$	1
		$2.2500 \times 10^9$	1
		$2.2438 \times 10^9$	1
		$2.4375 \times 10^9$	1
		$2.5313 \times 10^9$	1
		$2.6250 \times 10^9$	1
		$2.7188 \times 10^9$	1
		$2.8125 \times 10^9$	1
		$2.9062 \times 10^9$	2
		$3.0000 \times 10^9$	2

Table 6: Expansion points and moments matched for the clock tree  $n = 24566$

$tol = 1 \times 10^{-3}$		$tol = 1 \times 10^{-4}$	
expansion points	moments	expansion points	moments
0	4	0	4
$1.5000 \times 10^9$	4	$1.5000 \times 10^9$	3
$3.0000 \times 10^9$	4	$2.2500 \times 10^9$	3
		$3.0000 \times 10^9$	4
$tol = 1 \times 10^{-5}$		$tol = 1 \times 10^{-6}$	
expansion points	moments	expansion points	moments
0	1	0	1
$0.1875 \times 10^9$	1	$0.1875 \times 10^9$	1
$0.3750 \times 10^9$	1	$0.3750 \times 10^9$	1
$0.5625 \times 10^9$	1	$0.5625 \times 10^9$	1
$0.75 \times 10^9$	1	$0.7500 \times 10^9$	1
$0.9375 \times 10^9$	1	$0.9375 \times 10^9$	1
$1.1250 \times 10^9$	1	$1.1250 \times 10^9$	1
$1.3125 \times 10^9$	1	$1.3125 \times 10^9$	1
$1.5000 \times 10^9$	1	$1.5000 \times 10^9$	1
$1.6875 \times 10^9$	1	$1.6875 \times 10^9$	1
$1.8750 \times 10^9 j$	1	$1.7812 \times 10^9$	1
$2.0625 \times 10^9$	1	$1.8750 \times 10^9$	1
$2.2500 \times 10^9$	1	$1.9687 \times 10^9$	1
$2.4375 \times 10^9$	1	$2.0625 \times 10^9$	1
$2.6250 \times 10^9$	1	$2.2500 \times 10^9$	1
$2.8125 \times 10^9$	1	$2.4375 \times 10^9$	1
$3.0000 \times 10^9$	4	$2.5313 \times 10^9$	1
		$2.6250 \times 10^9$	1
		$2.7188 \times 10^9$	1
		$2.8125 \times 10^9$	1
		$2.8594 \times 10^9$	1
		$2.9062 \times 10^9$	1
		$2.9531 \times 10^9$	1
		$3.0000 \times 10^9$	1

Table 7: Expansion points and moments matched for the clock tree  $n = 24566$  (continued)

$tol = 1 \times 10^{-7}$		$tol = 1 \times 10^{-8}$	
expansion points	moments	expansion points	moments
0	1	0	2
$0.1875 \times 10^9$	1	$0.1875 \times 10^9$	2
$0.3750 \times 10^9$	2	$0.3750 \times 10^9$	2
$0.5625 \times 10^9$	2	$0.5625 \times 10^9$	2
$0.7500 \times 10^9$	2	$0.7500 \times 10^9$	2
$0.9375 \times 10^9$	2	$0.9375 \times 10^9$	2
$1.1250 \times 10^9$	2	$1.1250 \times 10^9$	2
$1.3125 \times 10^9$	2	$1.3125 \times 10^9$	2
$1.5000 \times 10^9$	2	$1.5000 \times 10^9$	2
$1.6875 \times 10^9$	2	$1.6875 \times 10^9$	2
$1.8750 \times 10^9$	2	$1.8750 \times 10^9$	2
$2.0625 \times 10^9$	2	$2.0625 \times 10^9$	2
$2.2500 \times 10^9$	2	$2.2500 \times 10^9$	2
$2.4375 \times 10^9$	2	$2.4375 \times 10^9$	2
$2.6250 \times 10^9$	2	$2.6250 \times 10^9$	2
$2.8125 \times 10^9$	2	$2.8125 \times 10^9$	2
$3.0000 \times 10^9$	2	$3.0000 \times 10^9$	2

Table 8: Expansion points and moments matched for the busline example  $n = 147$

$tol = 1 \times 10^{-3}$		$tol = 1 \times 10^{-4}$	
expansion points	moments	expansion points	moments
0	3	same as $tol = 1 \times 10^{-3}$	
$tol = 1 \times 10^{-5}$		$tol = 1 \times 10^{-6}$	
expansion points	moments	expansion points	moments
same as $tol = 1 \times 10^{-3}$		same as $tol = 1 \times 10^{-3}$	
$tol = 1 \times 10^{-7}$		$tol = 1 \times 10^{-8}$	
expansion points	moments	expansion points	moments
same as $tol = 1 \times 10^{-3}$		same as $tol = 1 \times 10^{-3}$	

Table 9: Expansion points and moments matched for the spiral inductor example  $n = 1434$

$tol = 1 \times 10^{-3}$		$tol = 1 \times 10^{-4}$	
expansion points	moments	expansion points	moments
0	3	0	4
$1.0000 \times 10^{10}$	3	$1.0000 \times 10^{10}$	4
$tol = 1 \times 10^{-5}$		$tol = 1 \times 10^{-6}$	
expansion points	moments	expansion points	moments
0	5	0	6
$1.0000 \times 10^{10}$	5	$1.0000 \times 10^{10}$	6
$tol = 1 \times 10^{-7}$		$tol = 1 \times 10^{-8}$	
expansion points	moments	expansion points	moments
0	4	0	4
$0.0158 \times 10^{10}$	3	$0.0158 \times 10^{10}$	4
$1.0000 \times 10^{10}$	3	$1.0000 \times 10^{10}$	4

Table 10: Expansion points and moments matched for the MIMO example  $n = 980$

$tol = 1 \times 10^{-3}$		$tol = 1 \times 10^{-4}$	
expansion points	moments	expansion points	moments
0	4	0	4
$3.0000 \times 10^9$	4	$3.0000 \times 10^9$	4
$tol = 1 \times 10^{-5}$		$tol = 1 \times 10^{-6}$	
expansion points	moments	expansion points	moments
0	3	0	3
$0.4218 \times 10^9$	3	$1.5000 \times 10^9$	3
$1.5000 \times 10^9$	3	$3.0000 \times 10^9$	3
$3.0000 \times 10^9$	3		
$tol = 1 \times 10^{-7}$		$tol = 1 \times 10^{-8}$	
expansion points	moments	expansion points	moments
0	3	0	5
$0.4218 \times 10^9$	3	$0.0067 \times 10^9$	1
$1.5000 \times 10^9$	3	$0.4218 \times 10^9$	1
$3.0000 \times 10^9$	3	$0.6913 \times 10^9$	1
		$0.9609 \times 10^9$	1
		$1.5000 \times 10^9$	1
		$1.8750 \times 10^9$	1
		$2.2500 \times 10^9$	1
		$2.6250 \times 10^9$	1
		$3.0000 \times 10^9$	1

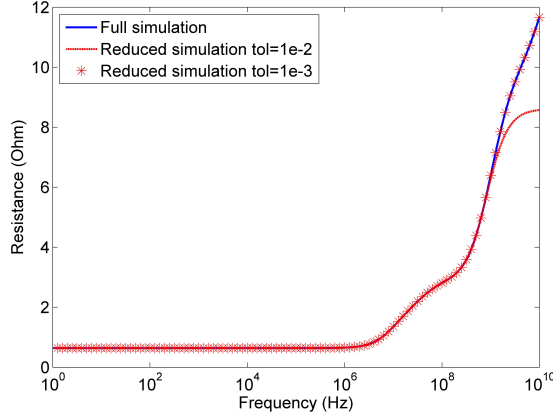


Figure 12: Resistance of the spiral inductor.

## 4.6 Comparison with PRIMA

We use the clock tree model with  $n = 24566$  and the spiral inductor model to compare our adaptive scheme with PRIMA. We set  $tol = 1 \times 10^{-5}$  and  $r_{max} = 20$  for both methods. In Fig. 15, the errors of the reduced transfer function of the clock tree model are compared. Our adaptive scheme uses 2 expansion points and the order of the reduced model is  $r = 18$ . The error is below  $tol = 1 \times 10^{-5}$ . If single expansion  $s_0 = s_l$  is used in PRIMA, and if  $q = 20$  moments are matched, the reduced model is of order  $r = 20$ , but with large error ( $\max_{s_i} e_R(s_i) = 0.8767$ ,  $s_i = 2\pi f_i$ ,  $i = 1, 2, \dots, 2000$  are the frequency samples) at high frequencies. If we increase the matched moments to  $q = 30$ , the reduced model of order  $r = 30$  has smaller errors, but is still not acceptable ( $\max_{s_i} e_R(s_i) = 0.015$ ). If using  $q = 40$  moments, the reduced model is of order  $r = 40$  and the accuracy is acceptable. However, the reduced model is more than double the size of the one derived by the adaptive scheme.

We compare the results for the spiral inductor in Fig. 16. Two expansion points  $s_0 = s_l$  and  $s_1 = s_h$  have been adaptively selected by our adaptive scheme. The resistance computed by the reduced model is indistinguishable from the results by full simulation. However if we use  $q = 15$ , and  $s_0 = s_l$  in PRIMA, the reduced model is of order  $r = 15$ , but with remarkably high error at high frequencies. Even if we increase  $q$  to  $q = 20$ , the reduced model with  $r = 20$  does not have the required accuracy.

## 5 Conclusions

A fully adaptive scheme for reduced order modeling of large scale linear time invariant systems is proposed. The adaptive scheme is based on a bisection principle for the interested frequency range. Given the desired accuracy and the acceptable order of the reduced model,

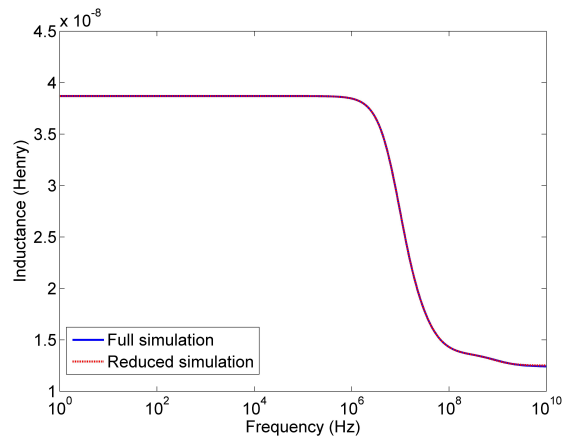


Figure 13: Inductance of the spiral inductor.

the adaptive scheme automatically generates the required reduced model by adaptively choosing the expansion points for the transfer function as well as the number of moments for each expansion point. If the given  $r_{max}$  is too small, the adaptive scheme can also automatically determine a proper order of the reduced model, which is kept as small as possible. The additional computations for the error control are reasonable. Various examples have been tested, which show the robustness of the adaptive scheme.

## Acknowledgment

We appreciate the many discussions with Prof. M. S. Nakhla and his nice suggestions. This work was supported by DFG grant BE 2174/7-1, Automatic, Parameter-Preserving Model Reduction for Applications in Microsystems Technology, by the BMBF-INUMAC project, and an operating grant of the University of Freiburg.

## References

- [1] B. C. Moore, "Principal component analysis in linear systems: Controllability, observability, and model reduction," *IEEE Trans. Automat. Control*, AC-26:17–32, 1981.
- [2] Peter Benner, "System-Theoretic Methods for Model Reduction of Large-Scale Systems: Simulation, Control, and Inverse Problems," *Proceedings of MathMod 2009*, Vienna, February 11-13, 2009, ARGESIM Report 35:126-145, 2009.
- [3] E. Chiprout and M. S. Nakhla, "Analysis of Interconnect Networks Using Complex Frequency Hopping (CFH)," *IEEE Trans. Comput.-Aided Des. Integr. Circuits Syst.*, 14(2): 186-200, 1995.

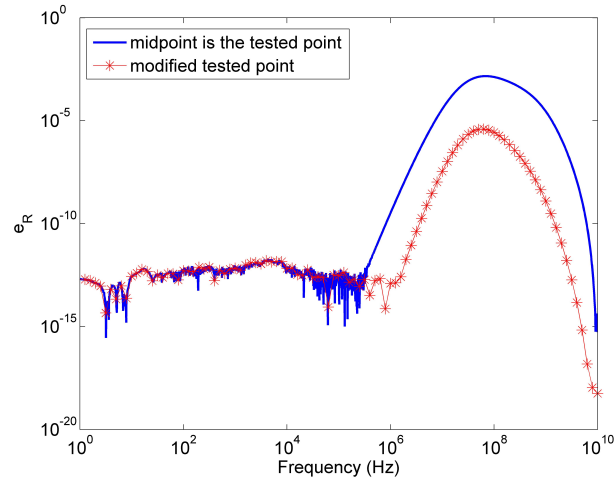


Figure 14: Error of the reduced transfer function with  $s_0 = s_l, s_1 = s_h$  for the spiral inductor with mid and modified tested point.

- [4] L. T. Pillage and R. A. Rohrer, "Asymptotic waveform evaluation for timing analysis", *IEEE Trans. Computer-Aided Design*, 9: 352-366, 1990.
- [5] R. Achar and M. S. Nakhla, "Simulation of high-speed interconnects," *Proceedings of the IEEE*, 89(5), 2001.
- [6] S. Gugercin, A. C. Antoulas, and C. A. Beattie, " $\mathcal{H}_2$  model reduction for large-scale linear dynamical systems," *SIAM J. Matrix Anal. Appl.*, 30(2): 609-638, 2008.
- [7] A. Odabasioglu, M. Celik, and L. T. Pileggi, "PRIMA: passive reduced-order interconnect macromodeling algorithm," *IEEE Trans. Comput.-Aided Des. Integr. Circuits Syst.*, 17(8):645-654, 1998.
- [8] P. Feldmann and R. W. Freund, "Efficient linear circuit analysis by Padé approximation via the Lanczos process," *IEEE Trans. Comput.-Aided Des. Integr. Circuits Syst.*, 14:639-649, 1995.
- [9] T. Bechtold, E. B. Rudnyi and J. G. Korvink, "Error indicators for fully automatic extraction of heat-transfer macromodels for MEMS," *Journal of Micromechanics and Microengineering*, 15(3):430-440, 2005.
- [10] T. Bui-Thanh, K. Willcox, and O. Ghattas, "Model Reduction for Large- Scale Systems with High-Dimensional Parametric Input Space", *SIAM Journal on Scientific Computing*, 30(6):3270-3288, 2008.

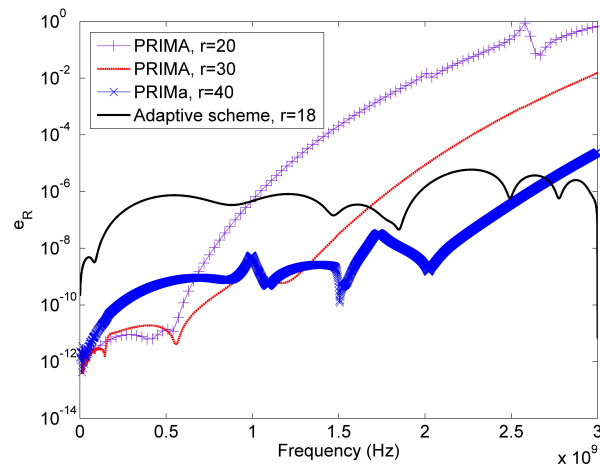


Figure 15: Comparison with PRIMA for the model of clock tree.

- [11] G. Rozza, D. B. P. Huynh, and A. T. Patera, “Reduced Basis Approximation and a Posteriori Error Estimation for Affinely Parametrized Elliptic Coercive Partial Differential Equations”, *Arch Comput Methods Eng*, 15:229-275, 2008. DOI 10.1007/s11831-008-9019-9
- [12] J.-R. Li, F. Wang, and J. White, “An efficient Lyapunov equation-based approach for generating reduced-order models of interconnect”, *In Proc. of 36th Design Automation Conference*, 1-6, 1999.

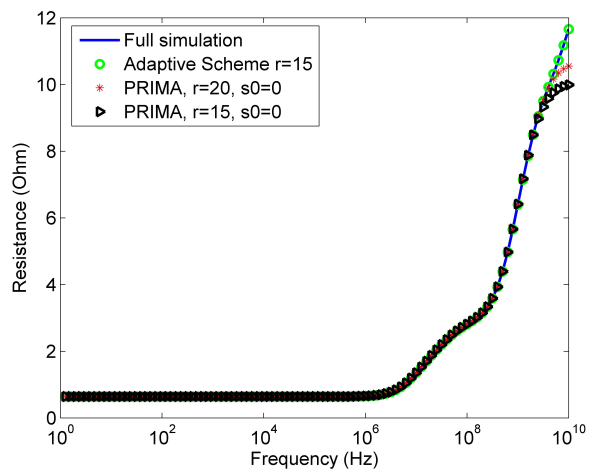


Figure 16: Comparison with PRIMA for the model of spiral inductor.

